HHS Public Access

Author manuscript

Air Qual Atmos Health. Author manuscript; available in PMC 2016 February 01.

Published in final edited form as:

Air Qual Atmos Health. 2015 February ; 8(1): 81–96. doi:10.1007/s11869-014-0276-5.

Influence of local meteorology and NO_2 conditions on ground-level ozone concentrations in the eastern part of Texas, USA

A. K. Gorai,

Environmental Science and Engineering Group, Birla Institute of Technology, Mesra, Ranchi 835215, India; Department of Technology, Jackson State University, Jackson, MS 39217, USA

F. Tuluri,

Department of Technology, Jackson State University, Jackson, MS 39217, USA

P. B. Tchounwou, and

NIMHD RCMI-Center for Environmental Health, Jackson State University, Jackson, MS 39217, USA

S. Ambinakudige

Department of Geosciences, Mississippi State University, Starkville, MS 39762, USA

Abstract

The influence of local climatic factors on ground-level ozone concentrations is an area of increasing interest to air quality management in regards to future climate change. This study presents an analysis on the role of temperature, wind speed, wind direction, and NO_2 level on ground-level ozone concentrations over the region of Eastern Texas, USA. Ozone concentrations at the ground level depend on the formation and dispersion processes. Formation process mainly depends on the precursor sources, whereas, the dispersion of ozone depends on meteorological factors. Study results showed that the spatial mean of ground-level ozone concentrations was highly dependent on the spatial mean of NO_2 concentrations. However, spatial distributions of NO_2 and ozone concentrations were not uniformed throughout the study period due to uneven wind speeds and wind directions. Wind speed and wind direction also played a significant role in the dispersion of ozone. Temperature profile in the area rarely had any effects on the ozone concentrations due to low spatial variations.

Keywords

Ground-level ozone; NO_2; Meteorology; Kriging; Mapping; Texas

Introduction

Increased air pollutant concentrations in the urban environment do not typically result from sudden increases in emissions, but rather from meteorological conditions that impede dispersion in the atmosphere or result in increased pollutant generation (Cheng et al. 2007).

amit_gorai@yahoo.co.uk.

There are many aspects of variations in air pollution that are still difficult to understand. One of these aspects is the estimation of the sensitivity of air pollutants to individual meteorological parameters. A combination of meteorological variables important to these conditions includes temperature, winds, radiation, atmospheric moisture, and mixing depth (US EPA 2009). It is well known that concentrations of pollutant within local air sheds are affected by meteorological parameters (Chung 1977; Elminir 2005; Ordonez et al. 2005; Cheng et al. 2007; Beaver and Palazoglu 2009). This has proven particularly challenging for several reasons. Primarily, meteorological parameters are inherently linked, resulting in strong interdependencies, for example, the dependency of atmospheric stability on temperature profile or the link between surface temperature and solar radiation. These associations make separating the effects of individual parameters a highly complex task. Further, meteorological parameters can affect pollutants through direct physical mechanisms such as the relationship with radiation and ozone or indirectly through influences on other meteorological parameters such as the association between high temperatures and low wind speed (Ordonez et al. 2005; Jacob and Winner 2009). Thus, multiple approaches are necessary to understand the true nature of meteorological pollutant relationships. To further complicate matters, the magnitude and nature of these effects can vary from one geographical region to the other due to differences in the topographical features. Additionally, the effects also changes across seasons, making site-specific assessments necessary for understanding local responses (Dawson et al. 2007; US EPA 2009).

One approach that has proven effective in measuring the effects of meteorological factors on air pollution is statistical modeling (Camalier et al. 2007). Statistical models are well suited for quantifying and visualizing the nature of pollutant response to individual meteorological parameters as they directly fit to the patterns that arise from the observed data (Schlink et al. 2006).

Ground-level ozone is a major component of smog. Photochemical reactions of volatile organic compounds (VOCs) and nitrogen oxides (NO_x) under high temperatures lead to ozone formation (Im et al. 2013; Seinfeld and Pandis 1998; Chung 1977). Often, NO_x alone controls the ozone formation, but increases with increasing VOC (Sillman et al. 1990; Im et al. 2013). The lifetime of the ozone depends on breaking of ozone and dispersions factors. Moreover, the spatial distribution of ozone concentrations is affected by precursor concentrations and the atmospheric conditions. Since source apportionment of O_3 is difficult as it is a secondary pollutant, and is not directly emitted from any source, it is imperative to accurately find the sources contributing to O_3 concentrations in urban areas in order to take corrective policy measures and develop cleaner technologies. Previous studies (Darby 2005; Pakalapati et al. 2009) investigated the influence of wind patterns on ozone concentrations in Houston, Texas, but did not assess the potential correlation between temperature and NO_2 which is considered to be a major precursor for ozone formation. Thus, a geographic information system (GIS)-based analysis was conducted for understanding the O_3 contributing factors (wind patterns, temperature, and NO_2 concentrations) in the proposed study area. Additionally, the mapping of ozone in urban areas assists the decision makers to describe and quantify its concentrations at locations where no measurement has been done and also to identify vulnerable areas for epidemiological studies. The preparation of maps is feasible if a spatial correlation of the variable of interest is identified (Hopkins et al. 1999).

The existence of a spatial correlation of air pollution is not only a condition for an optimum interpolation of the data in space in order to generate a map of ozone, but it also provides very useful insights on the formation and distribution processes. The overall objective of this research was to investigate the nature in which daily ozone concentrations respond to measures of local-scale meteorology and NO_2 concentrations in the eastern part of Texas, USA.

Materials and methods

Study area

The eastern part of Texas State (shown in the Fig. 1) was selected for the distribution analysis of ozone concentrations. Due to insufficient number of monitoring stations in the western part of the state, only the eastern part was considered for the study. The State of Texas is located in the west-south-central region of the USA. The longitude and latitude of the state are 71° 47′ 25″ W to 79° 45′ 54″ W and 40° 29′ 40″ N to 45° 0′ 42″ N, respectively. It is the second most populous (25,145,561), and the 29th most densely populated (96.3 inhabitants per square mile of land area) state of the 50 US States (U.S. Census Bureau: Resident population data 2010, http://www.census.gov/2010census/). Texas covers 261,797. 12 $mile^2$ of land area and ranks as the second largest state by size (U.S. Census Bureau, State area measurement, http://www.census.gov/geo/reference/state-area.html). In general, the climate in Texas varies widely, from arid in the west to humid in the east. The topography of Texas is characterized by the Gulf Coastal Plains of the eastern and southeastern part of the state, the North Central Plains of Central Texas, the Great Plains of the west–central region of Texas that extends to the Panhandle, and the hilly region of the Pecos area of the western side. The present study mainly covers the Gulf Coastal Plains due to significant variation in the geography from one region to another. There are coastal regions, mountains, deserts, and wide open plains. In coastal regions, the weather is neither particularly hot in the summer nor particularly cold during the winter. East Texas has the humid subtropical climate typical of the Southeast, occasionally interrupted by intrusions of cold air from the north.

Texas Commission on Environmental Quality (TCEQ) identified three zones for controlling NO_2 emissions from major combustion sources (source: https://www.tceq.texas.gov/airquality/stationary-rules/nox/major-sources). These are Beaumont/Port Arthur (BPA): Hardin, Jefferson, and Orange Counties; Dallas/Fort Worth (DFW): Collin, Dallas, Denton, Ellis, Kauffman, Johnson, Parker, Rockwall and Tarrant Counties; and Houston/Galveston/Brazoria (HGB): Harris, Galveston, Brazoria, Chambers, Fort Bend, Liberty, Montgomery, and Waller Counties. The three zones are marked in Fig. 1.

Data sources

As NO_2 and temperature play an important role in ozone formation, data on all three parameters were gathered. Ground-level ozone concentrations (daily maximum 8-h concentrations), and NO_2 concentrations (daily maximum 1-h concentrations) data monitored by US EPA were used in the study. Air pollution data collected by US EPA's air quality system (AQS) at the various monitoring stations located in different counties of the

eastern part of Texas for the 7-day period from May 1 to 7, 2012 were used for the study. The air pollution data used in this study was taken from the (U.S. EPA) air quality system data mart (Source: http://www.epa.gov/airdata/ad_rep_mon.html). The pollution concentrations of two criteria air pollutant parameters (NO_2 and O_3) at various monitoring stations located in different counties were retrieved for a 7-day period from May 1 to 7, 2012. Air pollution concentrations of NO_2 and ozone were obtained from 33 and 58 monitoring stations, respectively. The characteristics of the raw data collected from the website are daily maximum 8-h average concentrations of ozone and daily maximum 1-h average concentrations of NO_2. The pollutants were monitored as per the designated US EPA reference and equivalent methods. The details of the US EPA reference and equivalent methods are available in the website (http://www.epa.gov/ttnamti1/files/ambient/criteria/reference-equivalent-methods-list.pdf). The spatial locations (latitude and longitude) of each monitoring station were also obtained from the same source (source: http://www.epa.gov/airdata/ad_rep_mon.html). Generally, the highest ozone concentrations in urban areas were found in summer seasons. Hence, the duration for the present study was selected arbitrarily for 7 days (May 1 to 7, 2012) during the summer time. Temperature data along with the spatial locations at 49 monitoring stations were obtained from US EPA's offices on personal request. Statistical analyses were carried out for characterizing the data. Wind speed and wind direction data were obtained from the US Department of Agriculture's website (Source: http://www.wcc.nrcs.usda.gov/nwcc/site?sitenum=2016). The monitoring station is located in Waller county of Texas as shown in Fig. 1. The latitude and longitude of the location are 30° 5″ N and 95° 59″ W, respectively. Since the wind speed and wind directions data in multiple stations are not available or accessible in the study area, the wind characteristics are assumed to be uniformed in the regions.

Geostatistical (kriging) method for mapping

The sources of air pollution data for geographic information system (GIS) analysis were based on the measurements of air pollutant concentrations and temperature data that were routinely collected at 140 US EPA administered monitoring stations (33 for NO_2, 58 for ozone, and 49 for temperature) distributed in different counties as shown in Fig. 2. All point data (NO_2, O_3, and temperature) were entered into a GIS using ArcGIS software from Environmental Systems Research Inc. (ESRI). The first stage involved determining the location (latitude and longitude) of air pollution and temperature monitoring stations for the each station. The spatial locations of each of the selected monitoring stations along with the pollutant concentrations or temperature were fed into the GIS system for applying the kriging method for mapping. Kriging is a geostatistical method involving statistical techniques to analyze and predict spatial distribution pattern of a variable. It begins with a semivariance analysis, in which the degree of spatial autocorrelation is displayed as a variogram. Though, there are different types of kriging such as simple, ordinary, indicator, universal, disjunctive, and probability, the choice of a particular kriging method to use depends on the characteristics of the data and the type of spatial model desired. The most commonly used method is ordinary kriging, which was selected for this study because of its versatility and the limited application of other methods. Indicator kriging is used when it is desired to estimate a distribution of values within an area rather than just the mean value of

an area whereas universal kriging is used to estimate spatial means when the data have a strong trend and the trend can be modeled by simple functions. The method of kriging is briefly explained in this paper (for details see Yuval et al. 2005; Yuval and Broday 2006; Gorai and Kumar 2013). Kriging interpolation involves three steps: (i) exploratory analysis of data, (ii) structural analysis of data, and (iii) prediction and cross validation. Exploratory data analyses were performed to check data consistency and identify statistical distribution. Kriging methods work best for normally distributed data (Goovaerts 1997). The normality of the data for each day for three variables (ozone, NO_2, and temperature) was checked by Q–Q plot analyses [shown in Fig. 3a, c]. Transformations can be used to make the data normally distributed and satisfy the assumption of equal variability for the data. Q–Q plots analyses revealed that the data for each day for each variable were closely follow normal distribution. Thus, in the present study, no transformation of data was done for geostatistical analyses.

Structural analyses of data needed to determine the spatial correlations among data. Spatial correlation or dependence can be quantified with semivariograms (or simply known as variograms). Kriging relates the semivariogram, half the expected squared difference between paired data values $z(x)$ and $z(x+h)$ to the distance lag h, by which locations are separated. The basic function for semivariogram model for discrete sampling site is given in Eq. (1).

$$\gamma(h) = \frac{1}{2N(h)} \sum_{i=1}^{N(h)} [Z(X_i) - Z(X_i+h)]^2 \quad (1)$$

where $z(x_i)$ is the value of the variable z at location of x_i, h is the lag distance, and $N(h)$ is the number of pairs of sample points separated by h. For irregular sampling, it is rare for the distance between the sample pairs to be exactly equal to h. A semivariogram plot is obtained by calculating semivariance at different lags. These values are then usually fitted with a theoretical model (circular, spherical, exponential, Gaussian etc.). The models provide information about the spatial structure as well as the input parameters for the kriging interpolation. Stable semivariogram model were used for spatial prediction in each cases. Stable semivariogram model represents either the exponential or gaussian model depending on the optimum cross validation results.

The subsequent stage is the prediction of variables levels in unsampled locations. Predictive performances of the fitted models were checked on the basis of cross validation tests. The values of mean square error (MSE), and root mean square standardized error (RMSSE) estimated to ascertain the performance of the developed models. If the predictions are unbiased, the MSE should be near zero. RMSSE values should be close to one. If the RMSSE is greater than one, the variability of the predictions is underestimated; likewise if it is less than one, the variability is overestimated (ESRI 2003). After conducting the cross validation process, maps estimates from Kriging were generated, which provided a visual representation of the distribution of O_3, NO_2, and temperature. MSE and RMSSE are defined by the Eqs. (2)-(3).

$$MSE=\frac{1}{n}\sum_{i=1}^{n}\left[\hat{Z}\left(X_i\right)-Z\left(X_i\right)\right]/\hat{\sigma}\left(X_i\right) \quad (2)$$

$$RMSSE=\sqrt{\frac{1}{n}\sum_{i=1}^{n}\left[\frac{\left\{\left\{\hat{Z}\left(X_i\right)-Z\left(X_i\right)\right\}\right\}}{\hat{\sigma}\left(X_i\right)}\right]^2} \quad (3)$$

where $\hat{\sigma}^2\left(X_i\right)$ is the kriging variance for location X_i, $\hat{Z}\left(X_i\right)$ is predicted value and $Z(X_i)$ is the actual (measured) value at location X_i (Goovaerts 1997; Johnston et al. 2001).

All these analyses were carried out using Geostatistical Analyst module of ArcGIS software version 10.2.

Results and discussion

Variogram model analysis

To depict the distribution pattern of ozone, NO_2 and temperature in the study region, experimental semivariograms and their semivariogram models were first analyzed for each case. The cross validation results and the characteristics parameters of semivariogram models for each case are represented in Table 1. MSE for ozone prediction are 0.02, −0.04, 0, −0.01, 0.09, 0, and 0.03, respectively for 7 days (May 1 to 7, 2012). The respective values of RMSSE are 0.64, 0.76, 0.92, 0.81, 1.00, 0.64, and 0.83 for 7 days. The MSE values are close to zero and their corresponding RMSSE values close to one represent a good prediction model. The cross validation results indicate that MSE values closely followed the rule of thumb whereas the RMSSE values indicate that the predictions were overestimated in all the cases except one.

Similarly, MSE for NO_2 prediction are 0.07, 0.06, 0.03, 0.08, 0.05, 0.03, and 0.05, respectively, for 7 days (May 1 to 7, 2012). The respective values of RMSSE are 0.64, 0.76, 0.69, 0.81, 0.86, 0.88, and 0.75 for 7 days. In these cases also, the cross validation results indicate that MSE values closely followed the thumb rule whereas the RMSSE values indicate that the predictions were overestimated in all the cases.

The MSE for temperature prediction are 0.05, 0.02, −0.01, −0.001, 0.06, 0.07, −0.11, respectively, for 7 days (May 1 to 7, 2012). The respective values of RMSSE are 1.20, 1.26, 1.00, 1.09, 1.04, 1.32, and 1.28 for 7 days. The results indicate that MSEs are close to zero except in one case (May 7). On May 7, the MSE was relatively high. On the other hand, RMSSE values indicate that the predictions were underestimated in all the occasions.

The ratio of nugget variance to sill expressed in percentages can be regarded as a criterion for classifying the spatial dependence of ozone, NO_2, and temperature. The ratios were calculated for each case and represented in Table 1. If this ratio is less than 25 %, then the variable has strong spatial dependency; if the ratio is between 25 and 75 %, the variable has moderate spatial dependency, and if greater than 75 %, the variables shows only weak spatial dependency (Shi et al. 2007; Chien et al. 1997; Chang et al. 1998). The ratio

represented in Table 1 clearly indicate that ozone and temperature showed strong spatial structure in all cases. NO_2 showed strong spatial structure in four (May 1, May 2, May 5, and May 7) of the seven cases and moderate spatial structure in remaining cases.

The shape of the semivariogram was used to understand the spatial structures of ozone concentrations. Sill was used to quantify the variability of the ozone concentration among the sample sites. The sill (i.e., spatial variation) values in each case for ozone and NO_2 were significantly high. The sill values for temperature were found to be consistently low in each case except one (May 7).

Spatial distribution analysis

The spatial distribution of daily maximum 8-h ozone concentrations were examined using GIS and geostatistical techniques. Figure 4a and g depict the spatial patterns of daily maximum 8-h O_3 concentrations for 1 May 2012 to 7 May 2012, respectively. The descriptive statistics of the spatial distributions maps were determined using ArcGIS. The results are represented in Table 2. The mean ozone concentration in the area ranged from 32.99 ppb (May 3, 2012) to 59.56 ppb (May 1, 2012). The minimum ozone concentrations ranged from 17.24 ppb (May 5, 2012) to 26.03 ppb (May 7, 2012) and the maximum ozone concentrations ranged from 42.89 ppb (May 3, 2012) to 98.50 ppb (May 1, 2012). This clearly indicates that the variation in maximum concentrations is higher than the variations in minimum concentrations. This is due to the fact that the minimum ozone level is dominated by the existence of background ozone and the maximum ozone level is influence by formation and dispersion factors. Figure 4a, g indicate that the average/mean O_3 concentrations significantly declined from May 1 to 3 and then gradually increased until May 5. The mean concentrations remain at the same level in the next 2 days. The maximum concentrations in the 7-day period (during May 1 to 7, 2012) were observed, respectively, in the counties of Harris, Harrison, Grayson, Denton, Tarrant, Harris and Liberty. Figure 4a, g clearly indicate that the spatial trends of ozone concentrations were not uniformed in the study area during the period of May 1 to 7. This is due to frequent changes in the weather conditions in the regions. Therefore, the formation and dispersion of ozone have varied within the regions and thus showed no uniform spatial trend of ozone concentrations. The results of this study clearly illustrate the complex nature of spatial variation in ozone concentrations, and confirm the marked variation in dispersions and precursor's emissions characteristics.

Similarly, Fig. 5a, g show spatial distribution of daily maximum 1-h NO_2 concentrations from May 1 to 7, respectively. The mean NO_2 concentrations in the area ranged from 4.24 ppb (May 3, 2012) to 13.05 ppb (May 1, 2012). The minimum and maximum ozone concentrations ranged from 1.94 ppb (May 3, 2012) to 4.73 ppb (May 1, 2012) and 8.72 ppb (May 3, 2012) to 45.19 ppb (May 1, 2012), respectively. This clearly indicates that the variation in maximum concentrations is higher than the variations in minimum concentrations. This spatial pattern reflects most likely the aggregated density of emission source. Although no counties were exposed to "alert" (1-h maximum NO_2 guideline of US EPA, which is 100 ppb) levels during the 7 days (May 1 to 7, 2012), many counties in Beaumont/Port Arthur (BPA), Dallas/Fort Worth (DFW), and Houston/Galveston/Brazoria

(HGB) zones could be of some concern. The significant level of NO_2 was observed in the counties situated close to the three major emission zones (BPA, HGB, and DFW). The maximum NO_2 levels were observed in Harris county on May 1 to 4 and May 7. On May 5 and 6, the maximum levels were found in Dallas and Tarrant counties, respectively. Thus, it is clear from the exploratory data analyses that the major NO_2 emission sources situated on or near the Harris county.

The daily average temperature profiles for 7 days are shown in Fig. 6a, g. The spatial variation of temperature was relatively less. The mean temperatures in the area ranged from 75.28 °F (May 7, 2012) to 82.47 °F (May 3, 2012).

The graphical representations of the descriptive statistics for the three parameters are shown in Fig. 7a, c. These figures clearly indicate that the trend of mean ozone concentrations in the area followed the mean NO_2 concentrations during the 7-day period. But, the trends of these two pollutants did not match with the temperature variations in the area.

Correlation among ozone, temperature, and NO_2

Correlation analysis was done for quantifying the influence of temperature and NO_2 on ozone concentrations. Since the monitoring values of pollutant concentrations or temperature at common locations were not available, they were extracted from the interpolated maps using GIS. The values of ozone concentrations, NO_2 concentrations, and temperature at the centroid positions of each county (157 counties) were determined using spatial analyst tool of ArcGIS. The extracted data for 7 days (May 1 to 7, 2012) were used for correlation analyses. Pearson two-tailed correlation analyses were conducted using SPSS software version 21. Correlation analyses results of three variables in each day are represented in Table 3.

The results represented in Table 3 clearly indicate that NO_2 concentrations were significantly correlated with the ozone concentrations at 1 % significance level except on May 1 and 7, 2012. On May 1, the two variables were correlated at 5 % significance level. The correlation coefficients between ozone and NO_2 are 0.173, 0.683, 0.592, 0.302, 0.641, 0.452, and 0.091, respectively, for May 1 through 7. Since, all the correlation coefficients values are positive, it indicates that the higher concentrations of NO_2 level in the area increased the concentration of ozone.

Temperature did not show uniformed correlations with either NO_2 or ozone. The correlation coefficients between ozone and temperature were −0.387, −0.716, 0.534, 0.049, 0.406, −0.459, and 0.303, respectively, for May 1 to 7, 2012. The correlation coefficient results clearly indicate that ozone concentration was not influenced by temperature level in the area. Similarly, the correlation coefficients between NO_2 and temperature were −0.156, −0.425, 0.581, −0.375, 0.352, −0.569, and −0.120, respectively, for May 1 to 7. Again, the correlation coefficient result did not show any trend, that is, the values are negative in five occasions and positive in two occasions. Thus, the NO_2 concentrations in the study area may not be influenced by temperature level or some other factors playing a role in the observed differences in correlation coefficients.

Role of wind speed and wind direction on spatial distribution

Though the maximum NO_2 concentrations were observed near the emission sources in most instances, the locations of recorded maximum ozone concentrations varied with time. The prime reason behind this is the influence of wind speed and direction. The wind rose diagrams for 7-days period are shown in Fig. 8a, g. The wind rose diagrams were generated using WRPLOT View software version 7.0.0. Wind rose diagrams clearly indicate the significant fluctuation in wind speed and wind direction.

On May 1, 98.5 ppb of peak hour O_3 was observed in Harris county. This is due to maximum NO_2 level (45.19 ppb) also observed in the same county and the horizontal dispersion of NO_2 and ozone were relatively less as there was no particular dominant wind directions in that day. Easterly and south–easterly wind blowing in that day transported the ozone slowly in the south–east direction. Figure 5a clearly indicates the major sources of NO_2 are mainly in the regions HGB and DFW. The contribution of NO_2 from BPA was also significant.

On May 2, the maximum ozone concentration (68.66 ppb) was observed in Harrison county whereas the maximum NO_2 level (26.15 ppb) was observed in Harris county. The highest concentrations of NO_2 were observed in the counties situated close to the three major sources (BPA, HGB, and DFW). The top five counties, which showed maximum NO_2 levels, were Harris, Tarrant, Newton, Jasper, and Liberty. Three major sources of NO_2 mainly contribute to form high O_3 concentrations. The top five counties, where maximum ozone concentrations were observed, are Harrison, Marrion, Newton, Jasper, and Panola. Wind rose diagram clearly indicates that the prevailing wind directions were S to N and S–S–E to N–N–W. This leads to the significant transport of emissions from downwind urban and industrial areas, and thus the ozone concentrations were found to be maximum in the counties situated in the east and north east regions of the major pollution sources (Fig. 1).

On May 3, the maximum ozone concentration was observed in counties situated in the north–west region of the NO_2 emission sources. The wind rose diagram clearly indicates that the prevailing wind direction was S–S–E to N–N–W on May 3. Thus, the emissions of NO_2 in the regions HGB and BPA transported to north–west regions either after formation of ozone or in the same form. This process facilitates increase in the ozone concentrations in the counties Grayson, Cooke, Collin, Fannin, and Denton.

On May 4, the prevailing wind direction was same as that on May 3. But on May 4, the direction was more dominant and thus, the pollutants were transported to a greater extent in comparison to that on May 3. The spatial distribution map [Fig. 4d] of ozone clearly reveals that the ozone concentrations were found maximum in the N–W corner.

On May 5, there was no particular prevailing wind direction and thus the dispersion of NO_2 was not very significant. Spatial distribution maps of ozone on May 5 indicate that the maximum concentrations observed were close to the NO_2 emission sources.

On May 6, though the prevailing wind direction was S–S–E to N–N–W, the transportation of NO_2 was not significant due to lower frequency of wind in this direction in comparison to

that on May 2 and 4. Thus, the maximum NO_2 level was observed near to the emission sources and the secondary ozone dispersed in every direction of the emission sources.

On May 7, the maximum NO_2 concentration was found maximum near the emission sources but most of the time wind was blowing from N–E and N–W directions. This facilitates the dispersion of the secondary ozone towards the south. NO_2 emission in the region DFW dispersed towards the south and because of the low level of NO_2, no significant level of ozone was observed in the south of DFW. Higher level of ozone concentrations was observed in Liberty, Jefferson, Hardin, Harris, and Fortbend counties due to the transfer of NO_2 and ozone from the BPA region.

Conclusions

Ground-level ozone prediction and mapping have become an increasingly important part of air quality public outreach programs designed to inform the public about air quality conditions and protect public health. Exposure assessments that are only based on a small number of monitoring sites are likely to yield inaccurate results during epidemiological studies. Thus, understanding of the spatial distribution of ozone and identifying the underlying factors that affect its concentrations within an area of interest, is vital. GIS-based analysis was done for mapping and understanding the influence of NO_2, and local climatic conditions on ozone concentrations in Eastern Texas, USA. Study results indicated that ozone concentrations were highly correlated with NO_2 concentrations. Higher concentration levels of NO_2 were associated with higher concentrations of ozone. The distribution pattern of ozone was very much influenced by wind speed and wind direction but rarely showed any correlation with the temperature profile in the studied area. Hence, geospatial mapping of ozone provided a scientific basis for informed decision-making regarding the management of emission sources and control/prevention of ozone-related air pollution. This research also provided a basis to formulate new research hypotheses for further epidemiological studies regarding the health effects of air pollution in the studied area.

Acknowledgments

This research work was carried out in part of the corresponding author's Raman Postdoctoral Fellowship-2013 awarded by UGC, New Delhi, India. Authors are also thankful to US EPA for making air pollution data available on the website for public use. The support from the DST, New Delhi Grant No. SR/FTP/ES-17/2012, and the National Institutes of Health NIMHD Grant No. G12MD007581 through the RCMI-Center for Environmental Health at Jackson State University, are also acknowledged.

References

Beaver S, Palazoglu A. Influence of synoptic and mesoscale meteorology on ozone pollution potential for San Joaquin Valley of California. Atmos Environ. 2009; 43(10):1779–1788.

Camalier L, Cox W, Dolwick P. The effects of meteorology on ozone in urban areas and their use in assessing ozone trends. Atmos Environ. 2007; 41(33):7127–7137.

Chang YH, Scrimshaw MD, Emmerson RHC, Lester JN. Geostatistical analysis of sampling uncertainty at the Tollesbury managed retreat site in Blackwater Estuary, Essex, UK: kriging and cokriging approach to minimise sampling density. Sci Total Environ. 1998; 221:43–57.

Cheng CS, Campbell M, Li Q, Li G, Auld H, Day N, Pengelfly D, Gingrich S, Yap D. A synoptic climatological approach to assess climatic impact on air quality in south-central Canada. Part II: future estimates. Water Air Soil Poll. 2007; 182:117–130.

Chien YL, Lee DY, Guo HY, Houng KH. Geostatistical analysis of soil properties of mid-west Taiwan soils. Soil Sci. 1997; 162:291–297.

Chung YS. Ground-level ozone and regional transport of air pollutants. J Appl Meteorol. 1977; 16(11): 1127–1136.

Darby LS. Cluster analysis of surface winds in Houston, Texas, and the impact of wind patterns on ozone. J Appl Meteorol. 2005; 44:1788–1806.

Dawson JP, Adams PJ, Pandis SN. Sensitivity of ozone to summertime climate in the Eastern USA: a modeling case study. Atmos Environ. 2007; 41:1494–1511.

Elminir HK. Dependence of urban air pollutants on meteorology. Sci Total Environ. 2005; 350:225–237. [PubMed: 16227082]

ESRI. [accessed on December 2013] ArcGIS 9. Using ArcGIS Geostatistical Analyst: ONLINE. 2003. Available from: http://forums.esri.com/Thread.asp?c=93&f=1727&t=257926

Goovaerts, P. Geostatistics for natural resources evaluation. Applied geostatistics series. Oxford University Press; New York: 1997.

Gorai AK, Kumar S. Assessment of groundwater quality using statistical and geostatistical techniques in Ranchi Municipal Corporation Area, Jharkhand, India. Geoinfor Geostat: An Overview. 2013; 1(2) doi:10.4172/2327-4581.1000105.

Hopkins LP, Ensor KB, Rifai HS. Empirical evaluation of ambient ozone interpolation procedures to support exposure models. J Air Waste Manage Assoc. 1999; 49(7):839–846.

Im U, Incecik S, Guler M, Tek A, Topcu S, Unal YS, Yenigun O, Kindap T, Odman MT, Tayanc M. Analysis of surface ozone and nitrogen oxides at urban, semi-rural and rural sites in Istanbul, Turkey. Sci Total Environ. 2013; 443:920–931. [PubMed: 23247294]

Jacob DJ, Winner DA. Effect of climate change on air quality. Atmos Environ. 2009; 43(1):51–63.

Johnston K, Ver Hoef JM, Krivoruchko K, Lucas N. Using ArcGIS Geostatistical Analyst. 2001

Ordonez C, Mathis H, Furger M, Henne S, Hoglin C, Staehelin J, Prevot ASH. Changes of daily surface ozone maxima in Switzerland in all seasons from 1992 to 2002 and discussion of summer 2003. Atmos Chem Phys. 2005; 5:1187–1203.

Pakalapati S, Beaver S, Romagnoli JA, Palazoglu A. Sequencing diurnal airflow patterns for ozone exposure assessment around Houston, Texas. Atmos Environ. 2009; 43:715–723.

Schlink U, Herbarth O, Richter M, Dorling S, Nunnari G, Cawley G, Pelikan E. Statistical models to assess the health effects and to forecast ground-level ozone. Environ Model Softw. 2006; 21(4): 547–558.

Seinfeld, JH.; Pandis, SN. Atmospheric chemistry and physic from air pollution to climate change. Wiley; USA: 1998.

Shi J, Wang H, Xu J, Wu J, Liu X, Zhu H, Yu C. Spatial distribution of heavy metals in soils: a case study of Changxing, China. Environ Geol. 2007; 52(1):1–10. doi:10.1007/s00254-006-0443-6.

Sillman S, Logan JA, Wofry SC. A regional-scale model for ozone in the United States with a subgrid representation of urban and power plant plumes. J Geophys Res. 1990; 95(D5):5731–5748.

US EPA. Assessment of the impacts of global change on regional U.S. air quality: a synthesis of climate change impacts on ground-level ozone. US EPA; Washington, DC: 2009.

Yuval, Broday DM. High resolution spatial patterns of longterm mean air pollutants concentrations in Haifa Bay area. Atmos Environ. 2006; 40:3653–3664.

Yuval, Broday DM, Carmel Y. Mapping spatiotemporal variables: the impact of the time-averaging window width on the spatial accuracy. Atmos Environ. 2005; 39:3611–3619.

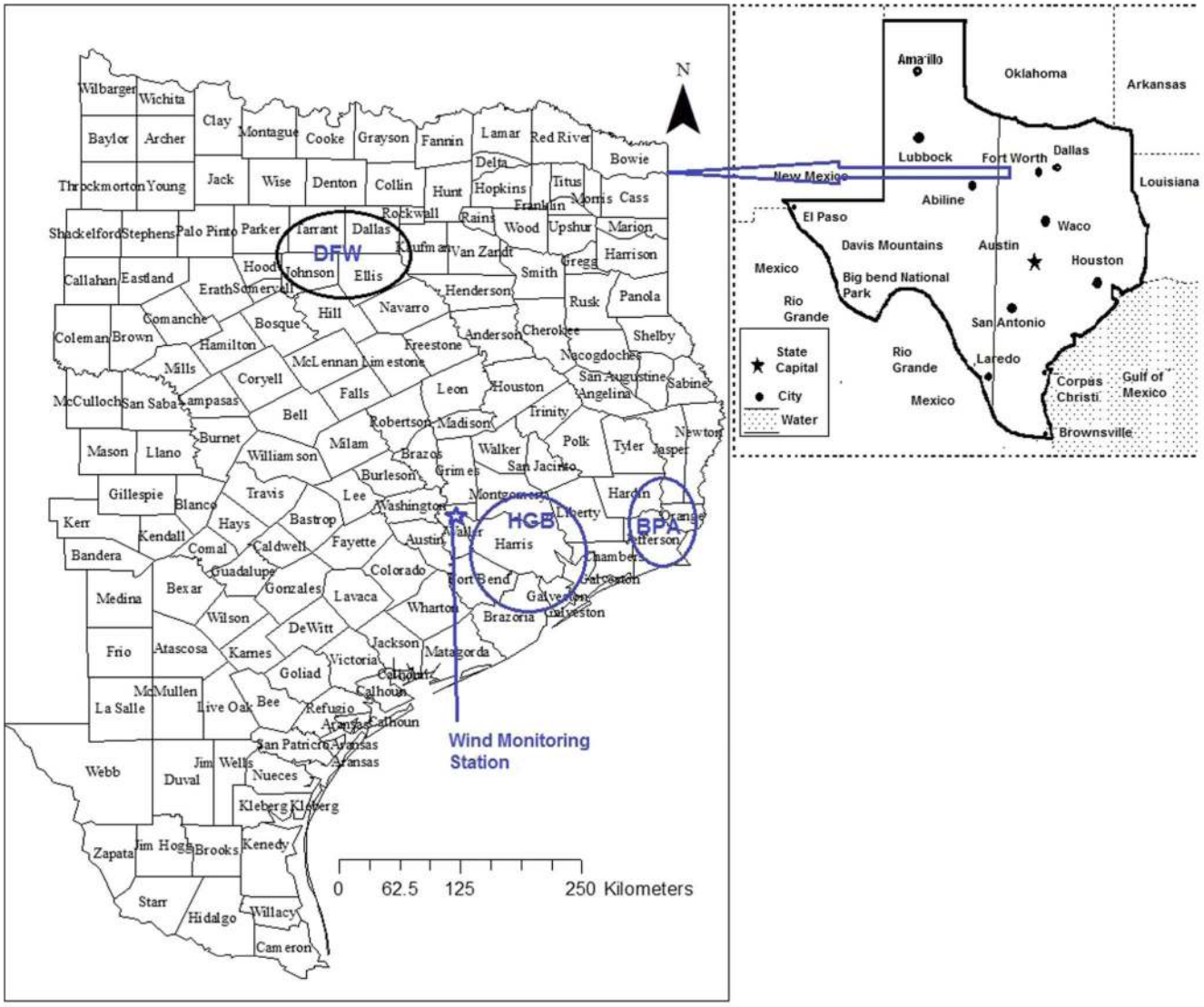

Fig. 1.
Study area map

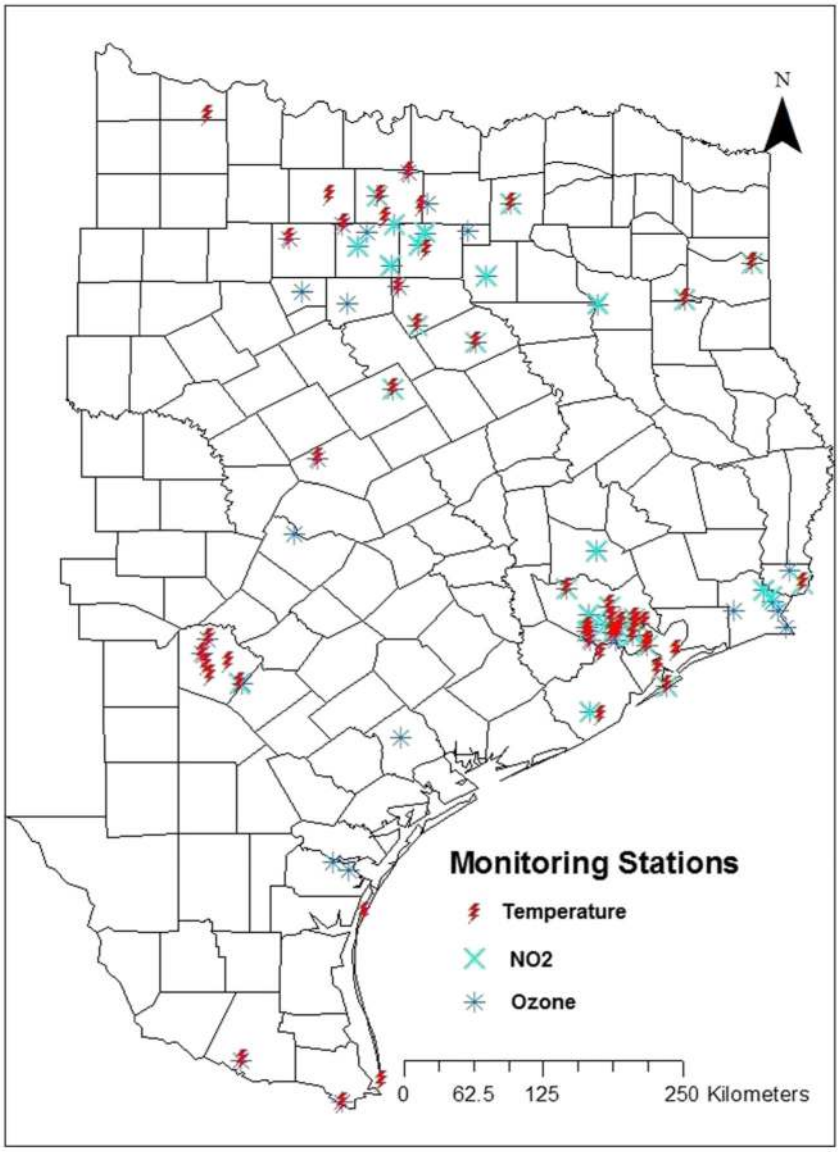

Fig. 2.
Air pollution and temperature monitoring stations

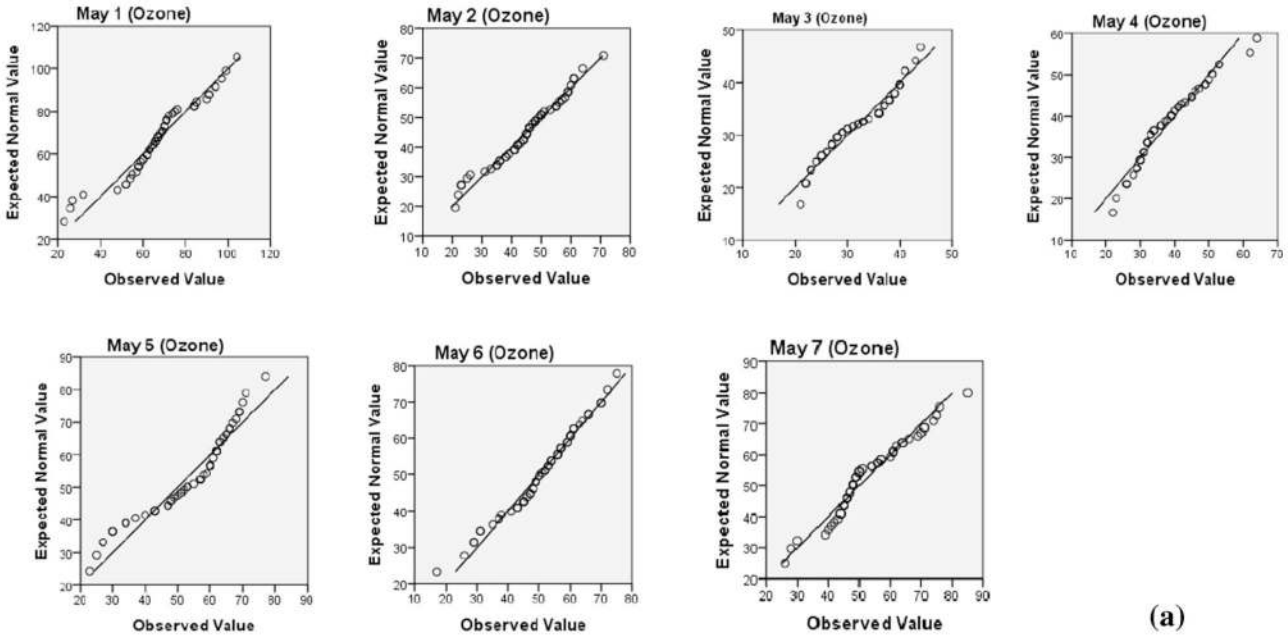

(a)

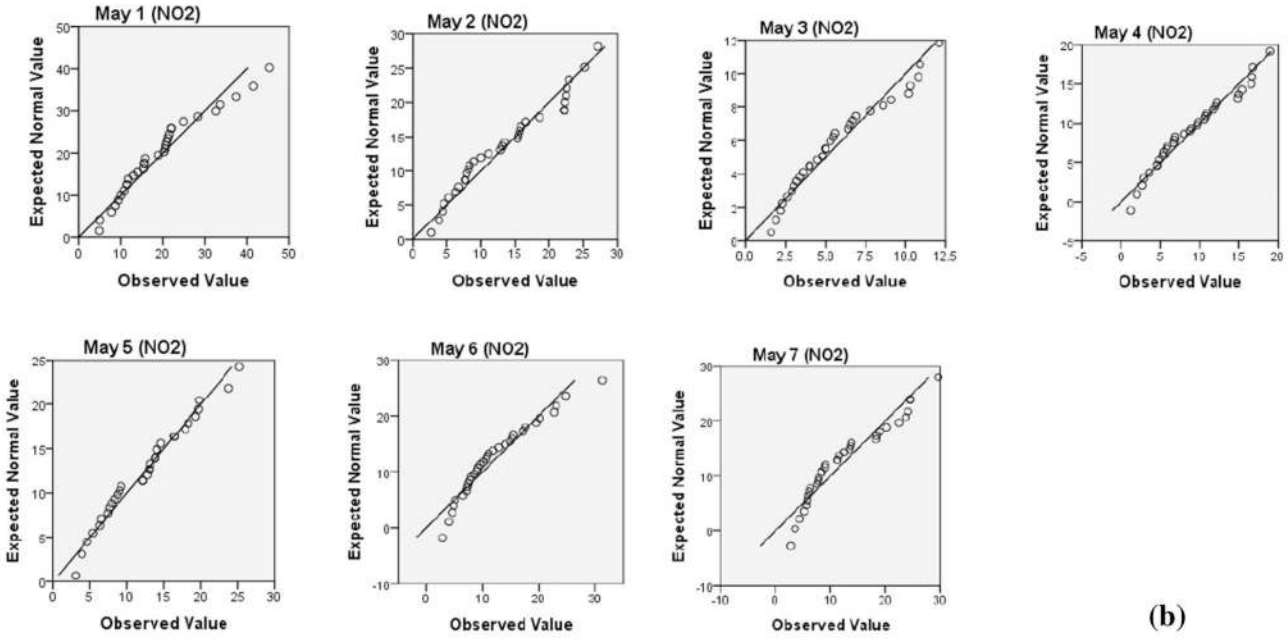

(b)

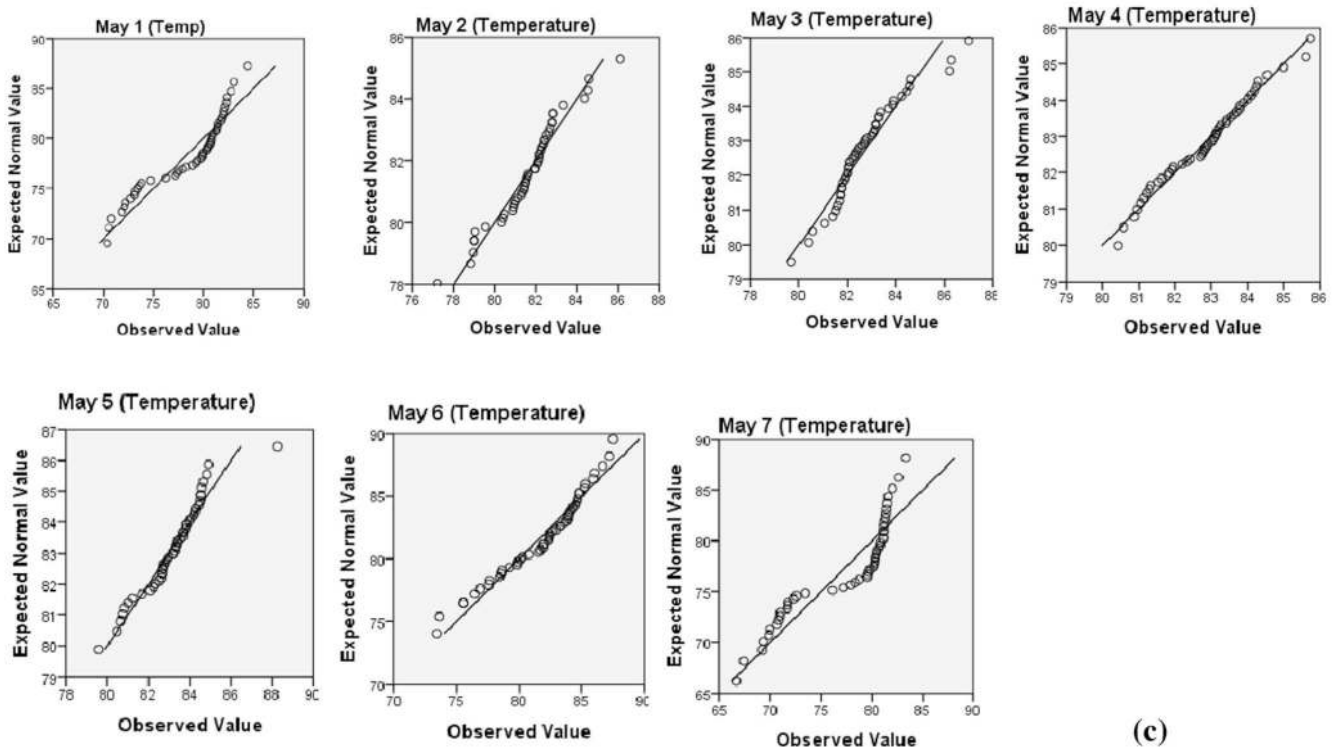

Fig. 3.

Q–Q plots of the three variables during the 7-day period from 1 May 2012 to 7 May 2012. **a** Ozone; **b** NO_2; **c** Temperature

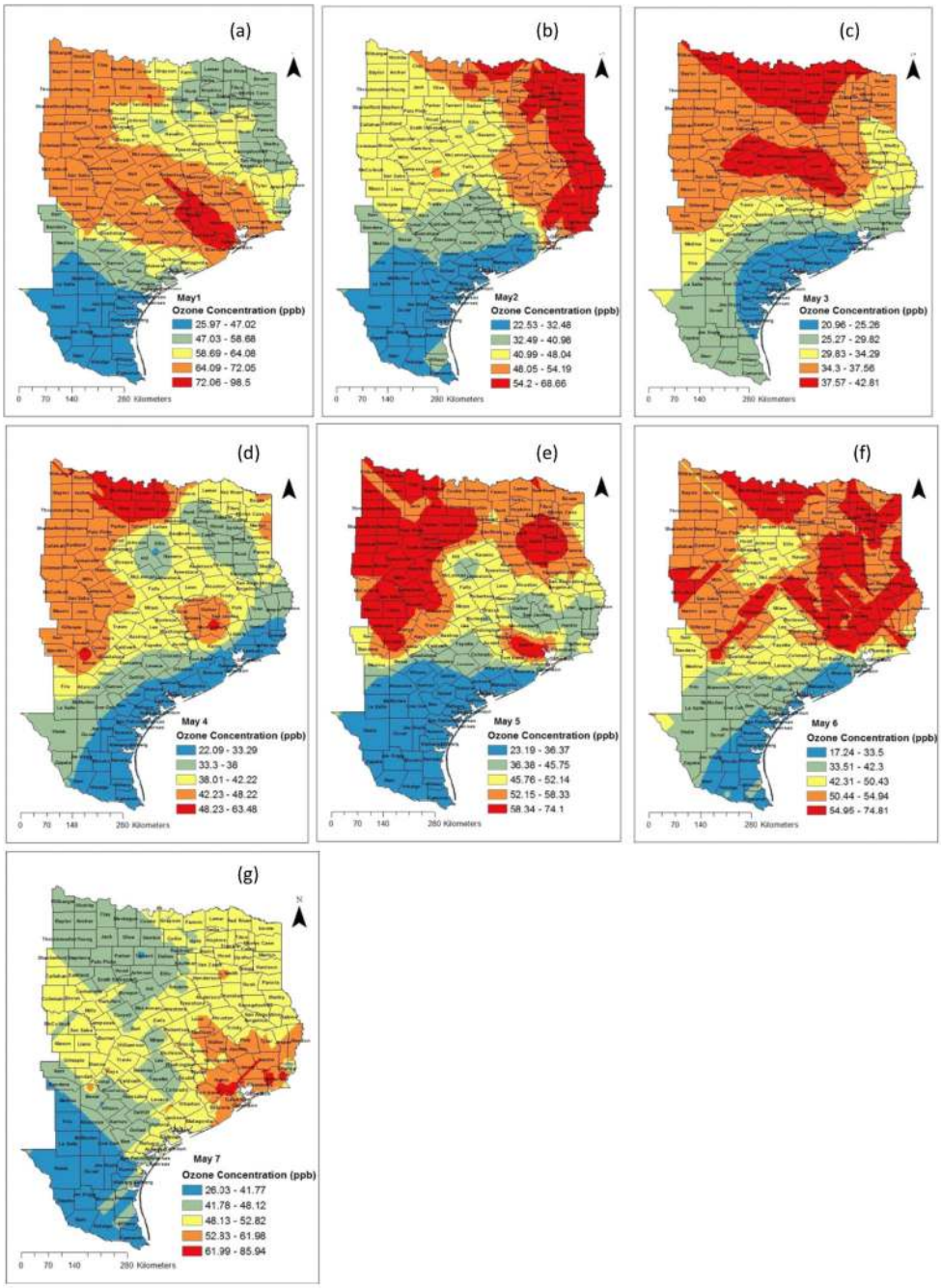

Fig. 4.

Spatial distribution of O_3 in the eastern part of Texas. **a** May 1, 2012; **b** May 2, 2012; **c** May 3, 2012; **d** May 4, 2012; **e** May 5, 2012; **f** May 6, 2012; **g** May 7, 2012

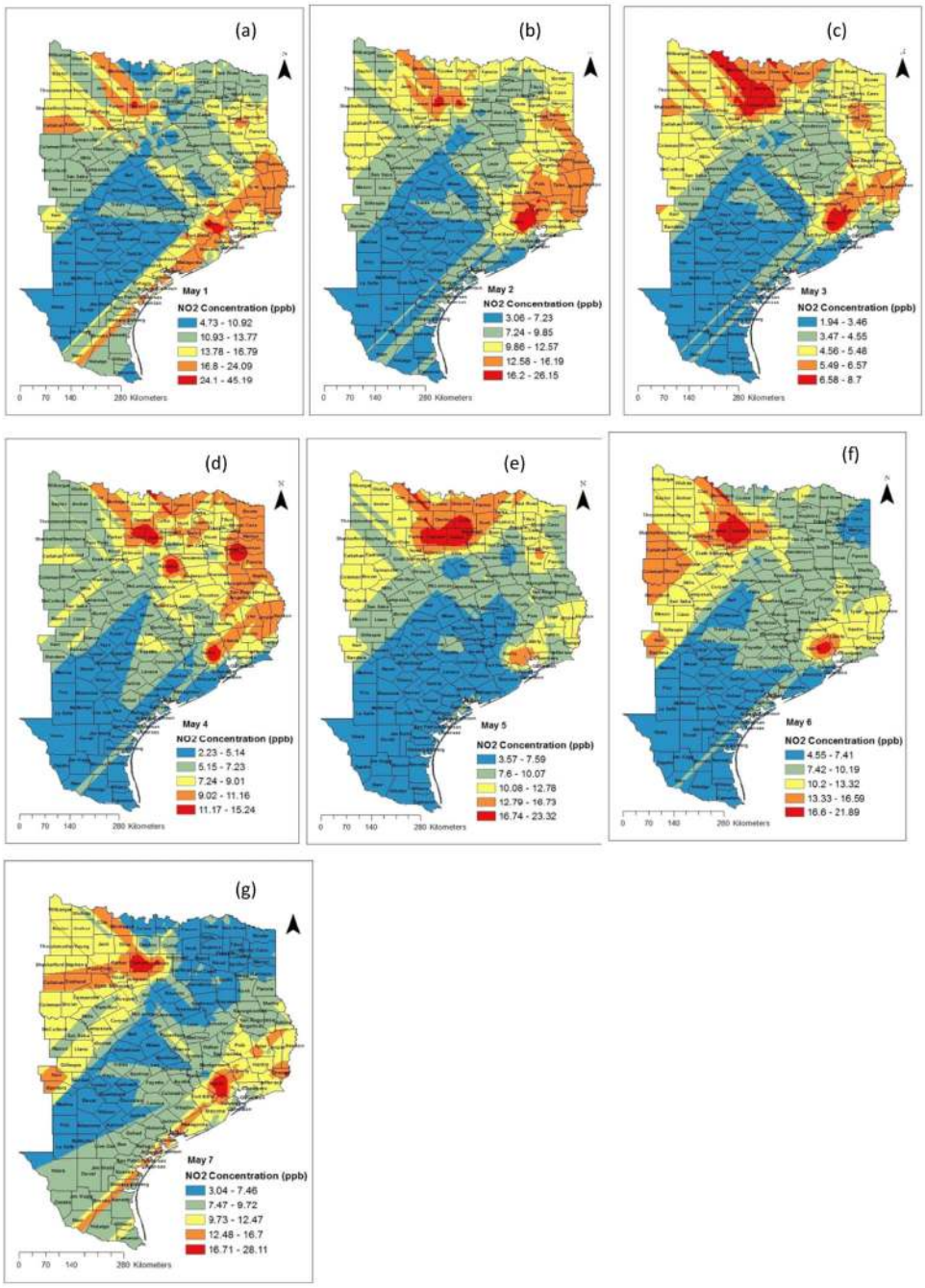

Fig. 5.

Spatial distribution of NO_2 in the eastern part of Texas. **a** May 1, 2012; **b** May 2, 2012; **c** May 3, 2012; **d** May 4, 2012; **e** May 5, 2012; **f** May 6, 2012; **g** May 7, 2012

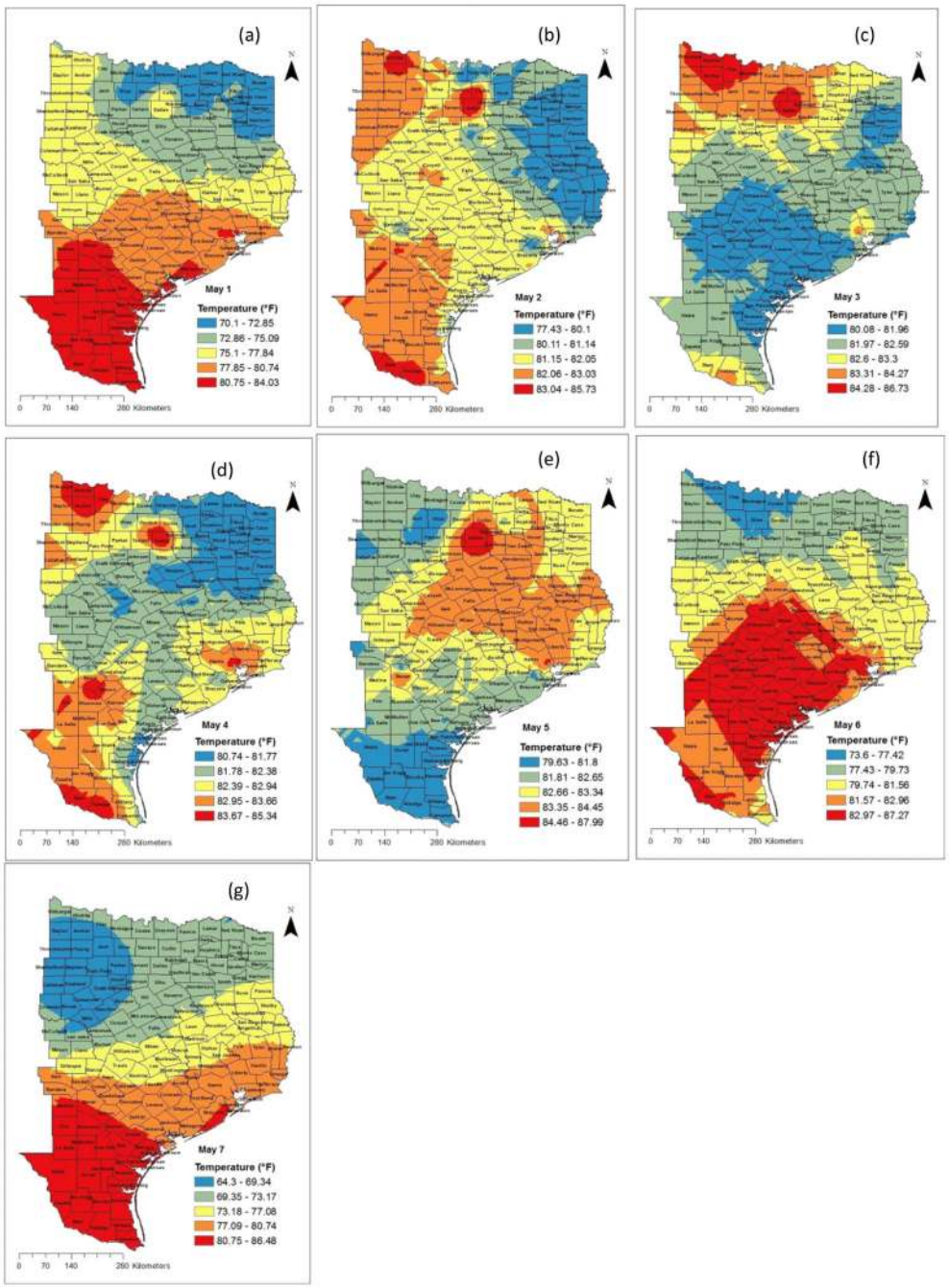

Fig. 6.

Temperature profile in the eastern part of Texas. **a** May 1, 2012; **b** May 2, 2012; **c** May 3, 2012; **d** May 4, 2012; **e** May 5, 2012; **f** May 6, 2012; **g** May 7, 2012

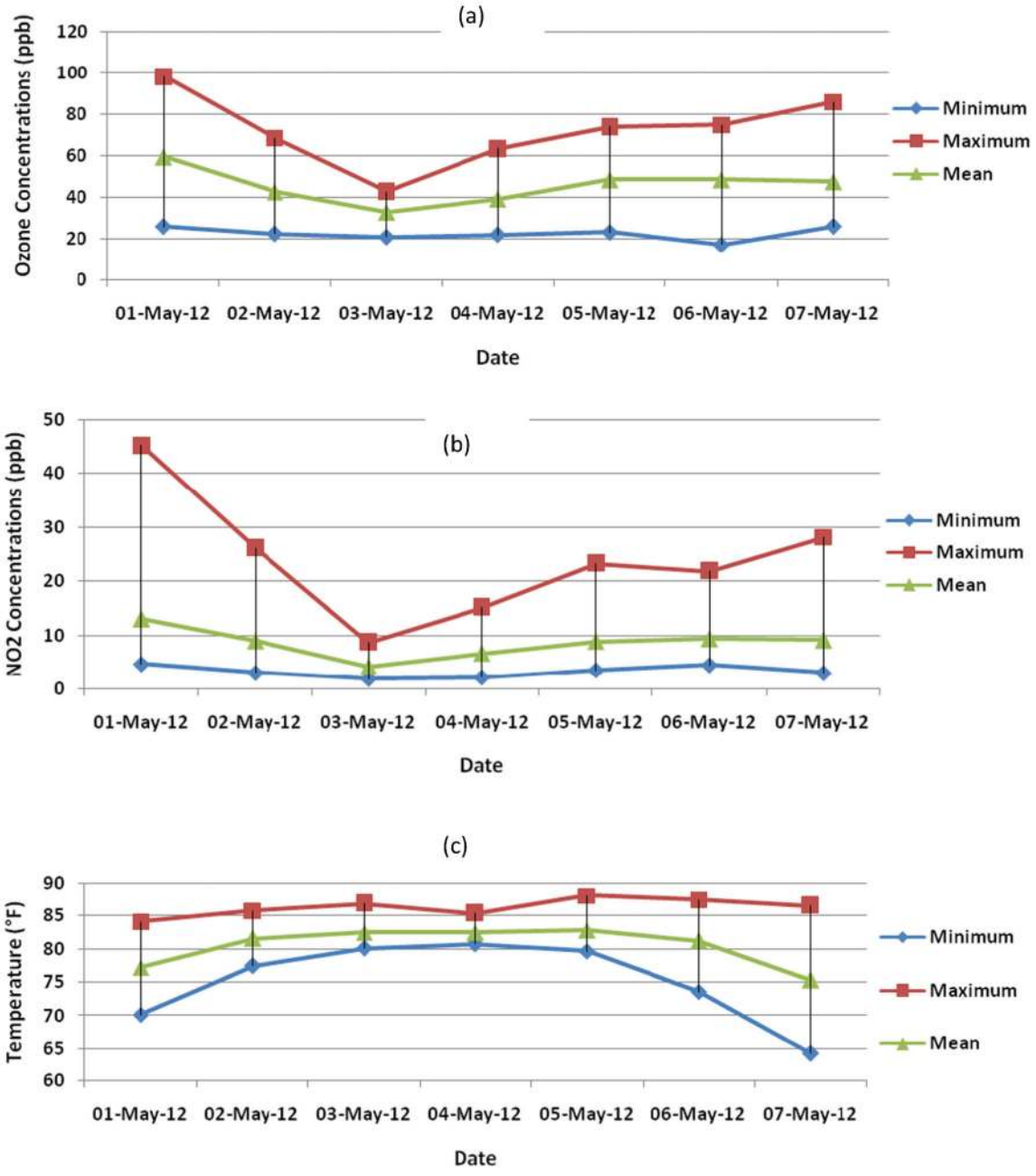

Fig. 7.

Graphical representations of the trend of NO_2, ozone, and temperature

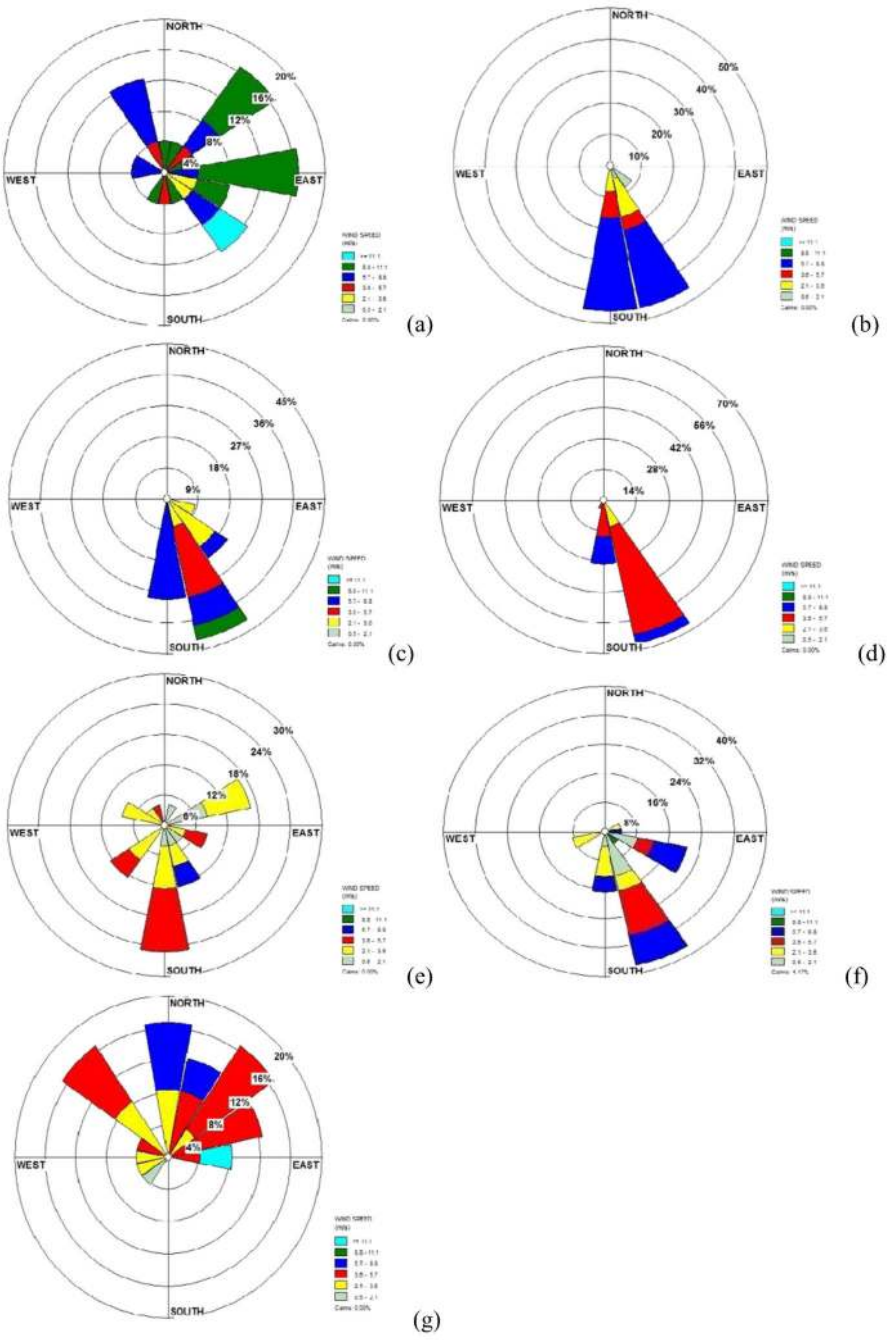

Fig. 8.

Wind rose diagram. **a** May 1, 2012; **b** May 2, 2012; **c** May 3, 2012; **d** May 4, 2012; **e** May 5, 2012; **f** May 6, 2012; **g** May 7, 2012

Table 1

Semivariogram model characteristics and cross validation results

Parameter	Fitted model	Nugget (C_0)	Partial sill (C)	[C0/(C0 + C)]%	Range	MSE	RMSSE
Ozone							
May 1,2012	Stable	0	169.7	0.0	1.20	0.02	0.64
May 2, 2012	Stable	15.16	52.15	22.5	0.53	−0.04	0.76
May 3, 2012	Stable	6.14	50.58	10.8	4.20	0.00	0.92
May 4, 2012	Stable	0	96.31	0.0	3.05	−0.01	0.81
May 5,2012	Stable	9.35	159.0	5.6	1.23	0.09	1.00
May 6, 2012	Stable	0	138.8	0.0	0.33	0.00	0.64
May 7, 2012	Stable	0.11	111.1	0.1	0.22	0.03	0.83
NO_2							
May 1, 2012	Stable	0.12	123.86	0.1	0.23	0.07	0.64
May 2, 2012	Stable	0	70.71	0.0	0.78	0.06	0.76
May 3, 2012	Stable	7.80	5.71	57.7	0.60	0.03	0.69
May 4, 2012	Stable	9.62	21.6	30.8	0.43	0.08	0.81
May 5,2012	Stable	6.64	37.93	14.9	0.83	0.05	0.86
May 6, 2012	Stable	28.47	33.28	46.1	0.71	0.03	0.88
May 7, 2012	Stable	0	75.63	0.0	0.64	0.05	0.75
Temperature							
May 1, 2012	Stable	0.55	3.18	14.7	1.05	0.05	1.20
May 2, 2012	Stable	0.29	1.55	15.8	0.53	0.02	1.26
May 3, 2012	Stable	0	1.82	0.0	1.54	−0.01	1.00
May 4, 2012	Stable	0.27	1.52	15.1	1.54	−0.001	1.09
May 5,2012	Stable	0	2.61	0.0	1.67	0.06	1.04
May 6, 2012	Stable	0	1.81	0.0	0.35	0.07	1.32
May 7, 2012	Stable	0.90	47.76	1.8	6.22	−0.11	1.28

Table 2

Descriptive statistics

Months	Number of data	Minimum	Maximum	Mean	Standard deviation
Ozone (ppb)					
May 1,2012	58	25.97	98.50	59.56	10.48
May 2, 2012	58	22.53	68.66	42.82	10.03
May 3, 2012	58	20.96	42.89	32.99	5.31
May 4, 2012	58	22.09	63.48	39.42	5.77
May 5,2012	58	23.19	74.10	48.57	11.85
May 6, 2012	58	17.24	74.81	48.60	8.80
May 7, 2012	58	26.03	85.94	47.73	5.58
NO2 (ppb)					
May 1, 2012	33	4.73	45.19	13.05	3.29
May 2, 2012	33	3.06	26.15	9.00	2.94
May 3, 2012	33	1.94	8.72	4.24	1.23
May 4, 2012	33	2.23	15.24	6.74	2.25
May 5,2012	33	3.57	23.32	8.93	3.06
May 6, 2012	33	4.55	21.89	9.40	3.06
May 7, 2012	33	3.04	28.11	9.17	2.64
Temperature (°F)					
May 1, 2012	49	70.10	84.09	77.18	3.44
May 2, 2012	49	77.43	85.73	81.49	1.13
May 3, 2012	49	80.08	86.75	82.47	0.82
May 4, 2012	49	80.74	85.34	82.44	0.73
May 5,2012	49	79.63	87.99	82.77	0.87
May 6, 2012	49	73.60	87.32	81.18	2.19
May 7, 2012	49	64.30	86.48	75.28	5.24

Table 3

Correlations coefficients among NO_2, ozone, and temperature

May 1				May 2			
	NO_2	Ozone	Temperature		NO_2	Ozone	Temperature
NO_2	1			NO_2	1		
Ozone	0.173*	1		Ozone	0.683**	1	
Temperature	−0.156	−0.387**	1	Temperature	−0.425**	−0.716**	1
May 3				May 4			
	NO_2	Ozone	Temperature		NO_2	Ozone	Temperature
NO_2	1			NO_2	1		
Ozone	0.592**	1		Ozone	0.302**	1	
Temperature	0.581**	0.534**	1	Temperature	−0.375**	0.049	1
May 5				May 6			
	NO_2	Ozone	Temperature		NO_2	Ozone	Temperature
NO_2	1			NO_2	1		
Ozone	0.641**	1		Ozone	0.452**	1	
Temperature	0.352**	0.406**	1	Temperature	−0.569**	−0.459**	1
May 7							
	NO_2	Ozone	Temperature				
NO_2	1						
Ozone	0.091	1					
Temperature	−0.120	−0.303**	1				

*Correlation is significant at the 0.05 level (2-tailed)

**Correlation is significant at the 0.01 level (2-tailed)